Intense Nonlinear Magnetic Dipole Radiation at Optical Frequencies: Molecular Scattering in a Dielectric Liquid

Samuel L. Oliveira* and Stephen C. Rand

Division of Applied Physics, University of Michigan, Randall Laboratory, Ann Arbor, Michigan 48109-1120, USA

(Received 15 June 2006; published 27 February 2007)

We report white-light generation and intense linear scattering from magnetic dipoles established by the time-varying magnetic flux of an incident light field in a dielectric medium. Large magnetic response is very unexpected at optical frequencies, and should lead to the discovery of new magneto-optical phenomena and the realization of low-loss homogeneous optical media with negative refractive indices.

DOI: 10.1103/PhysRevLett.98.093901 PACS numbers: 42.65.−k, 32.10.Dk, 78.20.Ci, 78.20.Ls

Since the time of James Clerk Maxwell [1] when the accumulated knowledge of electromagnetism was reduced to four compact equations, it has been widely recognized that the Lorentz force due to the magnetic field component of light is small. Hence, as electrons are linearly accelerated by the electric component of a light field, it has been generally assumed that their deflection by the magnetic component of the same field is negligible at nonrelativistic intensities ($\ll 10^{18}$ W/cm^2) in all types of matter. Equivalently, the time-varying flux of the optical magnetic field in atoms or molecules is not expected to produce enough electromotive force on charges to induce much circulation around the magnetic field at low intensities. In fact, Landau and Lifshitz stated that ''there is no meaning in using the magnetic susceptibility from optical frequencies onward, and in discussing such phenomena we must put $\mu = 1$'' [2]. Nevertheless, as shown both experimentally and theoretically in this Letter, the dynamic magnetic dipole moment generated by the passage of light can be fully half the electric dipole moment in nonmetals. The induced magnetic moment perpendicular to the electronic polarization can not only produce dipole radiation that is one fourth that produced by the electric field during linear optical interactions, but it can also result in intense nonlinear magneto-optic effects such as the magnetic dipole continuum emission reported here.

The existence of strong magnetic response at optical frequencies has important implications for linear and nonlinear optics alike. On the basis of the results reported here, it can be anticipated that numerous magnetic analogs of known nonlinear electro-optic phenomena remain to be discovered. In addition, since the present results show that nonresonant magnetic response can be very large even in nonmetals, magnetic resonance should be possible at optical frequencies. Resonant response would offer the prospect of tunable magnetic dispersion and negative permeability as needed to synthesize low-loss, homogeneous liquid or solid optical materials with negative refractive indices for ''perfect lenses'' [3], magnetic mirrors [4], nanolithography, and electromagnetic cloaking [5,6] in very simple ways.

As is well known, scattered electromagnetic fields in the radiation zone may be readily calculated using the expressions [7]

$$\mathbf{E}_{\text{rad}} = \frac{1}{4\pi\epsilon_0 c^2}\int \frac{([\dot{\mathbf{J}}]\times\hat{\mathbf{r}})\times\hat{\mathbf{r}}}{r}\,dv', \tag{1}$$

$$\mathbf{H}_{\text{rad}} = \frac{1}{4\pi c}\int \frac{[\dot{\mathbf{J}}]\times\hat{\mathbf{r}}}{r}\,dv', \tag{2}$$

where square brackets are evaluated at the retarded time. Here time derivatives are shown as dots, c is the velocity of light, and $\hat{\mathbf{r}}$ is a unit vector in the direction of the point of observation, at a distance r from the scattering volume. The prime on the differential volume indicates integration over the source distribution of charges. Knowledge of the vector current densities $\mathbf{J}_E$ and $\mathbf{J}_M$ associated with time-varying electric and magnetic dipole moments is enough to determine the electric and magnetic dipole components of light radiated from a sample. Since there are no magnetic charges, the magnetic current density $\mathbf{J}_M$ must derive from solenoidal motions of real charges.

We consider an incident plane wave that propagates along the z axis with its electric field linearly polarized along $\hat{\mathbf{x}}$ and its magnetic field oriented along $\hat{\mathbf{y}}$ (Fig. 1). In this classical picture, the wave impinges on a subwavelength spherical volume V corresponding to a particle, an atom or a molecule. Within the volume there is a uniform density of bound and free electrons all of which are assumed to respond to the fields, establishing polarization and conduction current densities $\mathbf{J}_p = \dot{\mathbf{P}}$ and $\mathbf{J}_c$, respectively. Although real currents are generally assumed to be parallel to the E field at low intensities, we allow for perpendicular components (along $\hat{\mathbf{z}}$) by writing all vector current densities that appear in Ampere's law

$$\boldsymbol{\nabla}\times\mathbf{H} = \varepsilon_0\dot{\mathbf{E}} + \mathbf{J}_c + \mathbf{J}_p + \mathbf{J}_M \tag{3}$$

as sums of a component parallel to $\mathbf{E}$ and a perpendicular component due to circulation around $\mathbf{B}$ governed by its time-varying flux:

 © 2007 The American Physical Society

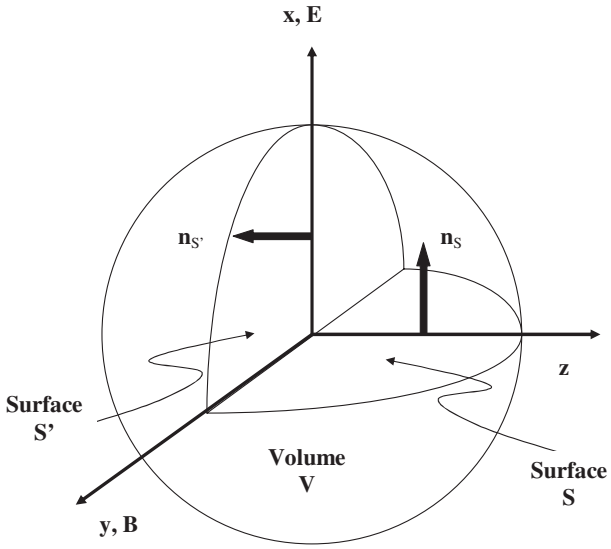

FIG. 1. Cross-sectional surfaces S and S' of a spherical volume containing bound and free electrons.

$$\mathbf{J}_M = \mathbf{J}_{M,\perp} + \mathbf{J}_{M,||}; \quad \mathbf{J}_c = \mathbf{J}_{c,\perp} + \mathbf{J}_{c,||}; \quad \mathbf{J}_p = \mathbf{J}_{p,\perp} + \mathbf{J}_{p,||}. \tag{4}$$

After substituting Eq. (4) into (3), an integration is performed over surface S in Fig. 1. Components perpendicular to $\mathbf{E}$ are orthogonal to the surface normal, hence one finds

$$\int_S (\nabla \times \mathbf{H}) \cdot d\mathbf{s} = \varepsilon_0 \int_S \dot{\mathbf{E}} \cdot d\mathbf{s} + \int_S \mathbf{J}_{c,||} \cdot d\mathbf{s} + \int_S \mathbf{J}_{p,||} \cdot d\mathbf{s} + \int_S \mathbf{J}_{M,||} \cdot d\mathbf{s}. \tag{5}$$

Assuming that all quantities vary sinusoidally at frequency ω, and using Faraday's law $\mathbf{H} = (\nabla \times \mathbf{E})/i\omega\mu_0$, one finds that the integral on the left of Eq. (5) is identical to the first on the right at high frequencies in regions of transparency. Hence Eq. (5) reduces to

$$\int_S \mathbf{J}_{M,||} \cdot d\mathbf{s} = -\int_S \mathbf{J}_{c,||} \cdot d\mathbf{s} - \int_S \mathbf{J}_{p,||} \cdot d\mathbf{s}. \tag{6}$$

A similar integration over surface S' in Fig. 1 yields

$$\int_{S'} \mathbf{J}_{M,\perp} \cdot d\mathbf{s} = -\int_{S'} \mathbf{J}_{c,\perp} \cdot d\mathbf{s} - \int_{S'} \mathbf{J}_{p,\perp} \cdot d\mathbf{s}. \tag{7}$$

By taking the divergence of Eq. (4) and combining it with the usual continuity of electric charge, a continuity condition for magnetic current $\mathbf{J}_M$ is easily derived in the form $\nabla \cdot \mathbf{J}_M = 0$. The divergence-free character of $\mathbf{J}_M$ assures us that the magnetic current component around the azimuth of the magnetic field is constant, or that $J_{M,\perp} = J_{M,||} = J_M$ in Eqs. (6) and (7). The addition of Eq. (6) and (7) therefore relates the magnitudes of magnetic and electric current densities according to

$$J_M = -\tfrac{1}{2}[J_c + J_p]_{\text{tot}}. \tag{8}$$

That is, the magnetic current density is minus one half the total current density due to real charge motion. The factor $\frac{1}{2}$ is the same as the ratio of magnetic (MD) to electric dipole (ED) moments of a perfectly conducting sphere in magnetostatics [8], but here it is obtained in a model that treats the transient response of conduction and bound electrons equivalently at optical frequencies. It follows immediately as a consequence of Eqs. (1) and (2) that the ratio of far-field MD to ED intensities calculated from the Poynting vector $\mathbf{S} = \mathbf{E} \times \mathbf{H}$ for sinusoidal fields is

$$\frac{S_M}{S_E} = \frac{1}{4}. \tag{9}$$

This classical result applies to conductors and insulators alike, to the extent that quantum-mechanical orbital constraints do not impede quasifree circulation of charges around $\mathbf{H}$, perpendicular to $\mathbf{E}$.

Ultrafast laser scattering experiments were performed with linearly polarized 150 fs pulses from a mode-locked and amplified laser system operating at 775 nm (Clark-MXR CPA-2001). A 90° scattering geometry was used and f8 focusing optics gave a confocal parameter of 0.4 m so that axial field amplitude from convergence of the wave was completely negligible ($E_z/E_0 \ll 10^{-3}$). To avoid damaging optical components, average power levels at 1 kHz repetition rate were maintained below 7 mW, corresponding to pulse energies <7 μJ and peak intensities at the focus of $I < 10^{13}$ W/cm^2. To map electric and magnetic dipole radiation patterns independently, transverse and axial polarization analysis was provided at the entrance to the detector (a cooled photomultiplier) in the plane transverse to the incident beam, as shown schematically in Fig. 2. A series of 10 nm passband interference filters was used to select the detection wavelength within the continuum spectrum generated by the sample. A liquid sample of pure carbon tetrachloride, prefiltered twice

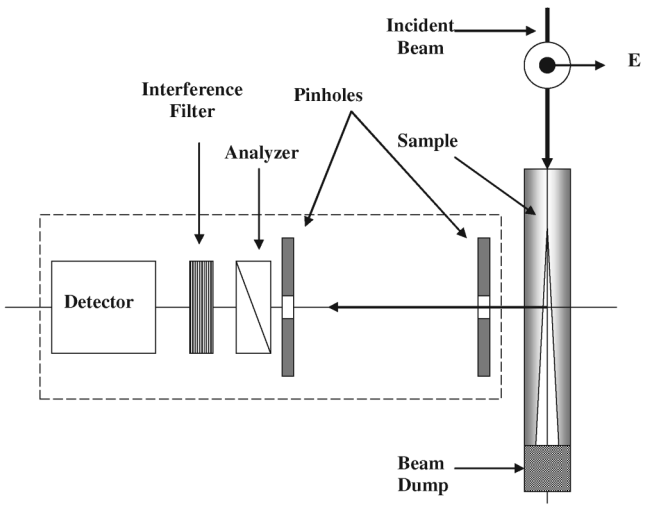

FIG. 2. Schematic diagram of the experimental geometry used to map electric and magnetic dipole radiation patterns by scanning polarization in the transverse plane of the incident light.

through a 0.2 μm mesh, was placed in a cylindrical glass holder and illuminated through the upper meniscus at room temperature. This transparent liquid sample is composed of totally symmetric molecules and was chosen both to eliminate possible magnetic interactions originating from conduction band electrons and those from scattering processes involving chirality or anisotropy of the sample. In anhydrous CCl_4, which is free of optical resonances (and therefore transparent) throughout the visible spectral range, the lack of particulate scattering or turbidity also precludes multiple scattering. Similar measurements were made in a horizontal scattering geometry using a rectangular sample cuvette and synchronous detection at the fundamental wavelength of a cw mode-locked Ti:Al_2O_3 laser (80 MHz repetition rate) focused to a peak intensity of $I = 2.2 \times 10^{10}$ W/cm^2.

The radiation patterns of scattered light were mapped using a double Fresnel rhomb placed in the input beam to rotate the incident polarization, keeping the detector fixed. The 90° scattering geometry was established within 30 arc sec, using an alignment laser and a precision right angle prism in place of the sample holder. Relative alignment of the incident beam with respect to all three axes of the apparatus was established by back propagation of He-Ne lasers over distances exceeding a meter. Two variable apertures of diameter ~3 mm, separated by 10 cm were used to select 90° scattered light and to reduce the relative signal contribution from out-of-plane electric dipole scattering associated with the finite detector solid angle to less than 10^{-4}.

In Fig. 3(a) the radiation patterns recorded from pure CCl_4 for axial and transverse polarizations are shown after subtraction of electronic noise (~30 counts/s). These results were obtained with amplified 775 nm pulses at a detection wavelength of 640 nm, slightly above the threshold for nonlinear white-light generation [9]. Results yielding the same ratio of magnetic to electric radiation were obtained at 390 nm and other test wavelengths within the continuum, including the fundamental wavelength 775 nm. Figure 3(b) shows that with unamplified pulses (having superior amplitude stability) similar results were obtainable below the threshold for white-light generation. Figure 3(c) is an enlargement of the axially polarized component in Fig. 3(b) that shows it is purely dipolar and orthogonal to the incident electric field. On an experimental basis alone, this is compelling evidence of magnetic dipole radiation. Ten measurements of the ratio of maximum magnetic to electric scattered intensities at 640 nm using amplified pulses gave an average of $S_M/S_E = 0.22 \pm 0.05$. This ratio was measured below the incident intensity at which multiple filaments formed, and was independent of detection aperture size in the range tested (<10 mm). No measurements were made in the multiple filament regime because of intensity fluctuations. The fit to low intensity data [Fig. 3(b)] similarly gave $S_M/S_E = 0.28 \pm 0.03$, and virtually identical results (not shown) were obtained in benzene and water.

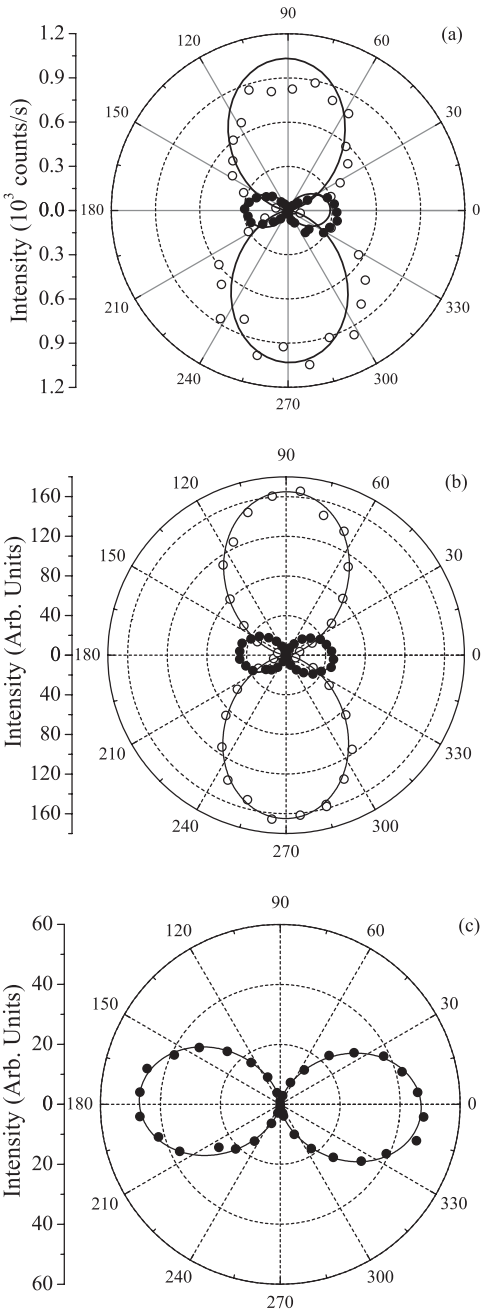

FIG. 3. Experimental far-field intensity patterns for axial (solid circles) and transverse (open circles) polarizations, measured using (a) amplified pulses ($\lambda_{in} = 775$ nm, $\lambda_{out} = 640$ nm, $I \sim 4.8 \times 10^{12}$ W/cm^2), and (b) unamplified pulses ($\lambda_{in} = 810$ nm, $\lambda_{out} = 810$ nm, $I \sim 2.2 \times 10^{10}$ W/cm^2) in CCl_4. (c) A magnified view of the null in the axial data of Fig. 3(b).

The solid curves in Fig. 3 are fits of $\sin^2\phi$ and $\cos^2\phi$ predictions for the azimuthal dependence of the orthogonal electric and magnetic contributions from transverse and axial dipolar elastic scattering, respectively. While good agreement between the theoretical curves and the data is

found, small systematic deviations are evident in data obtained with amplified pulses. This problem worsened at high incident power levels and was attributed to fluctuations in beam focusing and variations in the input beam position within the sample tube, which caused image displacement through the optical detection system during protracted 360° scans.

The magnetic dipole radiation in the data of Fig. 3 arises in the absence of any scattering particles other than the molecular scatterers themselves, and the measured values of S_M/S_E are in quantitative agreement with Eq. (9). However, the magnetic scattering is much more intense than expected from traditional predictions in the Rayleigh limit [8]. The second term of the multipole expansion predicts a relative magnetic dipole intensity of only $S_M/S_E \approx (v/c)^2 \approx (\lambda_c/a_0)^2 = 5.3 \times 10^{-5}$, where $\lambda_c = \hbar/mc$ is the Compton wavelength, a_0 is the Bohr radius, and m is the electron mass. However, this overlooks linear dipoles oriented perpendicular to the electric field in the first term of the expansion, which constitute magnetic dipole sources of the same order of magnitude as linear electric dipoles. We also note that in the present experiment the ratio of magnetic to electric dipole intensities for both nonlinear and linear scattering agrees with Eq. (9), even though, strictly speaking, the latter prediction applies only for nonresonant linear scattering. This is not coincidental, since at the location of a specified charge the local potential (whether linear or nonlinear) determines $\mathbf{J}_E$ and $\mathbf{J}_M$ simultaneously. Although restoring forces for orthogonal motions within the potential may be different, it is reasonable to expect that when the electric response becomes nonlinear in the applied field, the magnetic response becomes proportionately nonlinear. In the present experiments there is no evidence that the ratio of magnetic to electric scattering is affected by the nonlinear nature of the spectral redistribution of electromagnetic energy density that occurs during continuum generation. For all Fourier components of the continuum the ratio S_M/S_E is one quarter at high intensity.

Beam intensities in our experiments were far below levels required to accelerate electrons to the velocity of light during each optical cycle. Hence the intense magnetic scattering reported here is entirely nonrelativistic in nature. While the basic properties of carbon tetrachloride preclude explanations of magnetic or depolarized scattering based on multiple scattering, molecular chirality, static dipole alignment, anisotropy, or conductivity of the passive medium, the energy states of the electrons in our experiments nevertheless deserve careful consideration. Although CCl_4 itself is a dielectric, free electrons are reportedly generated above white-light threshold [9]. Hence free or nearly free electrons may contribute to the intense magnetic radiation in our amplified pulse data. Below white-light threshold, signals with both polarizations unfortunately rapidly approached the detection limit in experiments with the low repetition rate amplified laser system. The proportion of MD signal in relation to the ED signal was reliably determined for this linear scattering range only when 400 mW of output from a high repetition rate cw mode-locked $Ti:Al_2O_3$ laser was focused into CCl_4 with a 2 cm lens at a duty cycle of 50%. As shown in Fig. 3(b), this again yielded a ratio S_M/S_E equal to the predicted ratio $\frac{1}{4}$ within experimental error, showing that even linear scattering from CCl_4 at peak intensities below 10^{11} W/cm^2 in which no white-light or free electrons are generated can also yield the maximum MD response. However when a cw Argon laser was similarly focused into CCl_4 at 5×10^4 W/cm^2, no MD signal was detected at all. This suggests that quantum-mechanical constraints omitted from the classical treatment of magnetic response in Eq. (9) limit the solenoidal motion of electrons in ground state orbitals of CCl_4 at low intensities. However, the onset of delocalization perpendicular to $\mathbf{E}$ at higher intensities apparently mediates optical response with MD moments half as large as the ED moments, and might support optical magnetic resonance. A sufficiently large dispersion of the magnetic response can then result in a negative permeability at a small detuning from resonance where the medium is low-loss. Since it can be shown the permittivity will be simultaneously negative, the phase velocity of electromagnetic propagation will become negative. Consequently, this offers an approach to synthesizing a wide variety of unstructured, low-loss negative refractive media near optical resonances that may be tunable with external fields.

We acknowledge assistance from J. F. Whitaker and N. L. Sharma and partial research support from National Science Foundation Grants No. DMR-0502715 and No. CISE 0531086 and Air Force Office of Scientific Research Grant No. F49620-03-10389.

*Electronic address: samloliv@umich.edu

[1] J. C. Maxwell, Phil. Trans. R. Soc. Lond. **155**, 459 (1865).
[2] L. Landau and E. M. Lifshitz, *Electrodynamics of Continuous Media* (Pergamon Press, New York, 1984).
[3] J. B. Pendry, Phys. Rev. Lett. **85**, 3966 (2000).
[4] D. Sievenpiper, L. Zhang, R. F. J. Broas, N. G. Alexopolous, and E. Yablonovitch, IEEE Trans. Microwave Theory Tech. **47**, 2059 (1999).
[5] J. B. Pendry, D. Schurig, and D. R. Smith, Science **312**, 1780 (2006).
[6] D. Schurig, J. J. Mock, B. J. Justice, S. A. Cummer, J. B. Pendry, A. F. Starr, and D. R. Smith, Science **314**, 977 (2006).
[7] W. K. H. Panofsky and M. Phillips, *Classical Electricity and Magnetism* (Addison-Wesley, Reading, MA, 1962).
[8] J. D. Jackson, *Classical Electrodynamics* (Wiley, New York, 1975).
[9] A. Brodeur and S. L. Chin, J. Opt. Soc. Am. B **16**, 637 (1999).